Influence of Hydrogen-Bonding Substituents on the Cytotoxicity of RAPTA Compounds

Claudine Scolaro,[†] Tilmann J. Geldbach,[†] Sébastien Rochat,[†] Antoine Dorcier,[†] Christian Gossens,[†] Alberta Bergamo,[‡] Moreno Cocchietto,[‡] Ivano Tavernelli,[†] Gianni Sava,*[,‡,§] Ursula Rothlisberger,*[,†] and Paul J. Dyson*[,†]

Institut des Sciences et Ingénierie Chimiques, Ecole Polytechnique Fédérale de Lausanne (EPFL), CH-1015 Lausanne, Switzerland, Callerio Foundation Onlus, Via A. Fleming 22-31, 34127, Trieste, Italy, and Dipartimento di Scienze Biomediche, Università di Trieste, Via L. Giorgieri 7-9, 34127, Trieste, Italy

Received October 14, 2005

A new series of organometallic ruthenium(II)-arene compounds of the type $RuCl_2(\eta^6\text{-arene})$(phosphine) (phosphine = 1,3,5-triaza-7-phosphaadamantane, PTA, and 3,7-diacetyl-1,3,7-triaza-5-phosphabicyclo-[3.3.1]nonane, DAPTA) with different potential hydrogen-bonding functionalities on the arene ligand have been prepared and studied for their antitumor activity. Cell viability studies using the TS/A mouse adenocarcinoma cancer cell line and the nontumorigenic HBL-100 human mammary cell line, combined with uptake determinations, are compared to the nonfunctionalized analogues, previously shown to be active on solid metastasizing tumors. The reactivity of the functionalized RAPTA compounds with a 14-mer oligonucleotide (established by mass spectrometry) has been rationalized by DFT calculations, which indicate that environmental factors are important.

Introduction

Platinum compounds are widely used in the treatment of cancer with estimates indicating that 70% of all patients receive cisplatin during chemotherapy.[1−3] Despite the success of cisplatin and other platinum-based anticancer compounds in the clinic, there is still a need for new and improved anticancer drugs.[4,5] The need for new drugs is fuelled by the inability of platinum compounds to tackle some types of cancer of high social incidence and by the associated toxic side effects of the current platinum compounds in clinical use.[6]

The medicinal properties of the other platinum group metals are also well established, and one of the most promising metals in the treatment of cancer is ruthenium.[7] A number of ruthenium complexes show high in vitro and in vivo antitumor activity, and two compounds are currently undergoing clinical trials.[8,9] Like all metal drugs, the activity of the ruthenium compounds depends on both the oxidation state of the metal and the ligands coordinated to the center. Ruthenium also has unique properties that make it particularly useful in drug design, such as the biologically compatible ligand exchange kinetics of ruthenium(II) and ruthenium(III) compounds.[10,11] Ligand exchange is an important determinant of biological activity, as very few metal drugs reach their biological target without being modified. Moreover, ruthenium is unique among the platinum group metals in that the oxidation states Ru(II), Ru(III), and Ru(IV) are all accessible under physiological conditions. Ruthenium(III) complexes tend to be more biologically inert than related ruthenium(II) and ruthenium(IV) complexes, and in general, ruthenium compounds have a lower toxicity than their platinum counterparts. This lower toxicity is believed to be due to the ability of ruthenium to mimic iron in binding to many biological molecules, including serum transferrin and albumin, in particular taking advantage of the specific receptor-binding mechanism of transferrin.[12] Since rapidly dividing cells such as cancer cells have a greater requirement for iron, they increase the number of transferrin receptors located on their cell surface, thereby sequestering more of the circulating metal-loaded tranferrin, thus targeting a potential drug to the cancer cells and reducing the amount that reaches healthy cells.

Thus far, the majority of research centered on putative ruthenium drugs has focused on the antitumor activity of ruthenium coordination complexes.[13−15] More recently, organometallic ruthenium(II)-arene complexes of the type $RuCl_2(\eta^6\text{-benzene})$(metronidazole),[16] $RuCl_2(\eta^6\text{-arene})$(PTA),[17] [RuCl-

* To whom correspondence should be addressed. E-mail: paul.dyson@epfl.ch.

† EPFL.

‡ Callerio Foundation Onlus.

§ Università di Trieste.

(1) Barnard, C. F. J.; Cleare, M. J.; Hydes, P. C. *Chem. Br.* **1986**, *22*, 1001.

(2) Reedijk, J. *Chem. Commun.* **1996**, *7*, 801.

(3) Wong, E.; Giandomenico, C. M. *Chem. Rev.* **1999**, *99*, 2451.

(4) Cvitkovic, E.; Bekradda, M. *Semin. Oncol.* **1999**, *26*, 647.

(5) O'Dwyer, P. J.; Stevenson, J. P.; Johnson, S. W. *Drugs* **2000**, *59*, 19.

(6) Chu, G. *J. Biol. Chem.* **1994**, *269*, 787.

(7) Clarke, M. J.; Zhu, F.; Frasca, D. R. *Chem. Rev.* **1999**, *99*, 2511.

(8) Rademaker-Lakhai, J. M.; Van den Bongard, D.; Pluim, D.; Beijnen, J. H.; Schellens, J. H. M. *Clin. Canc. Res.* **2004**, *10*, 3717.

(9) Galanski, M.; Arion, V. B.; Jakupec, M. A.; Keppler, B. K. *Curr. Pharm. Des.* **2003**, *9*, 2078.

(10) Wang, F.; Chen, H.; Parsons, S.; Oswald, I. D. H.; Davidson, J. E.; Sadler, P. J. *Chem. Eur. J.* **2003**, *9*, 5810.

(11) Chatlas, J.; Van Eldik, R.; Keppler, B. K. *Inorg. Chim. Acta* **1995**, *233*, 59.

(12) (a) Srivastava, S. C., Mausner, L. F.; Clarke, M. J. *Progress in Clinical Biochemistry and Medicine−Non-Platinum Metal Complexes in Cancer Chemotherapy*; Clarke, M. J., Ed.; Springer-Verlag: Berlin, 1989; p 111. (b) Srivastava, S. C.; Richards, P.; Meinken, G. E.; Larson, S. M.; Grunbaum, Z. In *Radiopharmaceuticals: Structure Activity Relationship*; Spencer, R., Ed.; Grune and Stratton: New York, 1981; p 207.

(13) Keppler, B. K.; Lipponer, K. G.; Stenzel, B.; Kratz, F. *Met. Complexes Cancer Chemother.* **1993**, 187.

(14) Sava, G.; Bergamo, A. *Int. J. Oncol.* **2000**, *17* (2), 353.

(15) Alessio, E.; Mestroni, G.; Bergamo, A.; Sava, G. *Met. Ions Biol. Syst.* **2004**, *42*, 323.

(16) Dale, L. D.; Tocher, J. H.; Dyson, T. M.; Edwards, D. I.; Tocher, D. A. *Anti-Cancer Drug Des.* **1992**, *7*, 3.

10.1021/om0508841 CCC: $33.50
Publication on Web 12/31/2005

Scheme 1. Synthesis of Ruthenium(II)-Arene Compounds 1−4

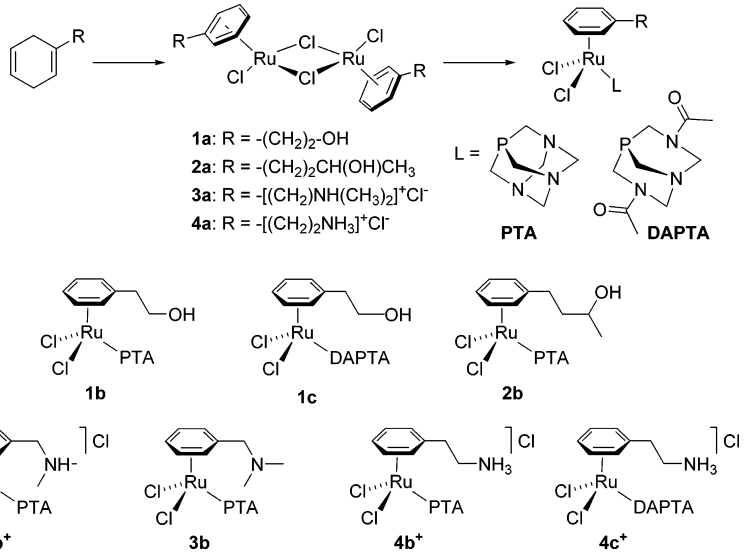

(η^6-arene)(en)]$^+$ (en = ethylenediamine),[18] and $RuCl_2(\eta^6$-$C_6H_6)(Me_2SO)$[19] and compounds with related sulfur ligands,[20] as well as a series of compounds that evaluate the necessity of the arene ring, viz., replacing the arene with a sulfur macrocycle or pentamethylcyclopentadienyl ligand,[21] have been studied for their antitumor activity in vitro and in some cases in vivo. The ethylenediamine series of complexes, [RuCl(η^6-arene)(en)]$^+$, have been evaluated for activity both in vitro and in vivo in human ovarian cancer, and show high activity coupled to non-cross-resistance in cisplatin-resistant models.[22] The PTA series of compounds were shown to be active toward the TS/A mouse adenocarcinoma cancer cell line, whereas no cytotoxicity on the HBL-100 human mammary (nontumorigenic) cell line was observed, which indicates selectivity of these ruthenium(II)-arene complexes to cancer cells.[23] In vivo, $RuCl_2(\eta^6$-*p*-cymene)-(PTA) (RAPTA-C) and $RuCl_2(\eta^6$-benzene)(PTA) (RAPTA-B) were found to be inactive against primary tumors, but were effective at reducing the growth of lung metastases in CBA mice bearing the MCa mammary carcinoma and also showed excellent clearance rates from the vital organs and low general toxicity. Other types of organometallic drugs[24] include titanocene compounds,[25] although clinical trials were recently discontinued,[26] and ferrocene (and other organometallic) derivatives of selective estrogen receptor modulators such as tamoxifen, which show considerable promise against various types of hormone-related cancers.[27]

The mechanism of activity of the RAPTA compounds remains elusive, but the traditional target for many metal-based drugs is usually considered to be DNA. It is well established that cisplatin binds to DNA involving coordination and H-bonding interactions, and combined, these interactions prevent protein synthesis and replication, leading to cell death.[28] One potential way to increase the activity of a compound that can coordinate to DNA is to include hydrogen-bonding functionalities on the compound such that both coordination and hydrogen-bonding interactions with DNA can occur. Such a strategy has previously been applied to titanocene drugs, and increased cytotoxicities were indeed found.[29] In this paper we evaluate a similar strategy, attaching hydrogen-bonding substituents to the arene ligand of the RAPTA antitumor complexes in an attempt to increase their cytotoxicity, and we attempt to correlate activity with uptake and DNA binding. Additionally, the effect of changing the phosphine ligand to PTA-related ligands is also explored.

Results and Discussion

A series of RAPTA compounds bearing functionalized η^6-arene ligands with potential hydrogen-bonding substituents were prepared according to the procedure depicted in Scheme 1. Starting from the appropriate functionalized arene, the corresponding diene is prepared via Birch reduction,[30] and subsequent reaction with ruthenium(III) chloride in methanol under reflux affords the dinuclear chloro-bridged ruthenium complexes.[8] Addition of PTA or DAPTA in either DMF or a mixture of

(17) Allardyce, C. S.; Dyson, P. J.; Ellis, D. J.; Heath, S. L. *Chem. Commun.* **2001**, 1396.
(18) Chen, H.; Parkinson, J. A.; Morris, R. E.; Sadler, P. J. *J. Am. Chem. Soc.* **2003**, *125*, 173.
(19) Gopal, Y. N. V.; Jayaraju, D.; Kondapi, A. K. *Biochemistry* **1999**, *38*, 4382.
(20) Huxham, L. A.; Cheu, E. L. S.; Patrick, B. O.; James, B. R. *Inorg. Chim. Acta* **2003**, *352*, 238.
(21) (a) Akbayeva, D. N.; Gonsalvi, L.; Oberhauser, W.; Peruzzini, M.; Vizza, F.; Brueggeller, P.; Romerosa, A.; Sava, G.; Bergamo, A. *Chem. Commun.* **2003**, 264. (b) Serli, B.; Zangrando, E.; Gianferrara, T.; Scolaro, C.; Dyson, P. J.; Alessio, E. *Eur. J. Inorg. Chem.* **2005**, *17*, 3423.
(22) Aird, R. E.; Cummings, J.; Ritchie, A. A.; Muir, M.; Morris, R. E.; Chen, H.; Sadler, P. J.; Jodrell, D. I. *Br. J. Cancer* **2002**, *86*, 1652.
(23) Scolaro, C.; Bergamo, A.; Brescacin, L.; Delfino, R.; Cocchietto, M.; Laurenczy, G.; Geldbach, T. J.; Sava, G.; Dyson, P. J. *J. Med. Chem.* **2005**, *48* (12), 4161.
(24) Allardyce, C. S.; Dorcier, A.; Scolaro, C.; Dyson, P. J. *Appl. Organomet. Chem.* **2005**, *19*, 1.
(25) Köpf-Maier, P.; Köpf, H. *Arzneimittel-Forschung* **1987**, *37*, 532.
(26) (a) Kröger, N.; Kleeberg, U. R.; Mross, K.; Edler, L.; Hossfeld, D. K. *Onkologie* **2000**, *23*, 60. (b) Mross, K.; Robben-Bathe, P.; Edler, L.; Baumgart, J.; Berdel, W. E.; Fiebig, H.; Unger, C. *Onkologie* **2000**, *23*, 576.
(27) (a) Top, S.; Kaloun, E. B.; Vessières, A.; Leclercq, G.; Laïos, I.; Ourevitch, M.; Deuschel, C.; McGlinchey, M. J.; Jaouen, G. *ChemBioChem* **2003**, *4*, 754. (b) Top, S.; Kaloun, E. B.; Vessières, A.; Laïos, I.; Leclercq, G.; Jaouen, G. *J. Organomet. Chem.* **2002**, *643*−*644*, 350. (c) Top, S.; Vessières, A.; Pigeon, P.; Rager, M.-N.; Huché, M.; Salomon, E.; Cabestaing, C.; Vaissermann, J.; Jaouen, G. *ChemBioChem* **2004**, *5*, 1104. (d) Top, S.; Vessières, A.; Leclercq, G.; Quivy, J.; Tang, J.; Vaissermann, J.; Huché, M.; Jaouen, G. *Chem. Eur. J.* **2003**, *9*, 5223. (e) Pigeon, P.; Top, S.; Vessières, A.; Huché, M.; Hillard, E. A.; Salomon, E.; Jaouen, G. *J. Med. Chem.* **2005**, *48*, 2814. (f) Vessières, A.; Top, S.; Beck, W.; Hillard E.; Jaouen, G. *Dalton Trans.* **2005**, in press, online.
(28) (a) Takahara, P. M.; Rosenzweig, A. C.; Frederick, C. A.; Lippard, S. J. *Nature* **1995**, *277*, 649. (b) Jamieson, E. R.; Lippard, S. J. *Chem. Rev.* **1999**, *99*, 2467. (c) Wang, D.; Lippard, S. J. *Nat. Rev. Drug Discovery* **2005**, *4*, 307.
(29) Rehmann, F.-J. K.; Cuffe, L. P.; Mendoza, O.; Rai, D. K.; Sweeney, N.; Strohfeldt, K.; Gallagher, W. M.; Tacke, M. *Appl. Organomet. Chem.* **2005**, *19*, 293.
(30) Kuehne, M. E.; Lambert, B. F. *J. Am. Chem. Soc.* **1959**, *81*, 4278.

Scheme 2

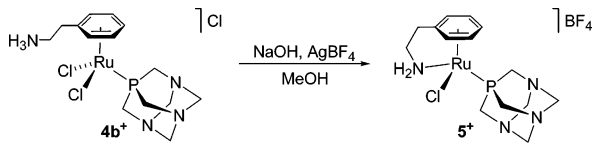

$MeOH/CH_2Cl_2$ leads to the formation of the corresponding ruthenium(II)-arene complexes **1**−**4**.

Deprotonation of **4b**$^+$ with a strong base and subsequent chloride abstraction with $AgBF_4$ affords the cationic complex **5**$^+$, as shown in Scheme 2. Full synthetic and spectroscopic details of these compounds are provided in the Experimental Section; the numbering scheme for the NMR data is given in the Supporting Information.

All complexes have been fully characterized by NMR spectroscopy, electrospray ionization mass spectrometry (ESI-MS), and elemental analysis. The presence of either an amine or alcohol functionality does not exert a marked effect on the carbon atoms of the coordinated arenes, as evidenced by ^{13}C NMR spectroscopy in DMSO-d_6. Likewise, the ^{31}P chemical shift remains essentially unaffected, being observed around −33 ppm for the PTA complexes **1b**−**4b**$^+$ and **5**$^+$ and around −12 ppm for the DAPTA complexes **1c** and **4c**$^+$. In the ESI mass spectra, the most prominent signal stems either from the parent ion, $[M]^+$, for the naturally charged compounds **3b**$^+$, **4b**$^+$, **4c**$^+$, and **5**$^+$ or from chloride loss, $[M - Cl]^+$, for the neutral complexes **1b**, **1c**, **2b**, and **3b**. The structure of **5**$^+$ has been established in the solid state by single-crystal X-ray diffraction and is discussed later.

Cytotoxicity of 1−5 on Cells and Drug Uptake Studies. The MTT test was carried out on compounds **1**−**5** using the tumor mouse TS/A cell line and the human HBL-100 cell line, which is a model for nontumorigenic cells, previously used to evaluate the activity of other RAPTA compounds.[23] The effects of **1**−**5** on the growth of these cells were evaluated after 24, 48, and 72 h treatment, and the results from the tumor mouse TS/A cell studies are displayed in Figure 1. The experiments were repeated twice for all the compounds, and the corresponding IC_{50} values resulting from an average of the two experiments are listed in Table 1 for both cell types.

From Table 1 it can be seen that complexes **4c**$^+$ and **5**$^+$ are nontoxic toward the TS/A adenocarcinoma cell line. For these two complexes the IC_{50} values exceed the maximum concentration used for the MTT experiments, viz., 1000 μM. It is noteworthy that, despite the presence of the functional groups that might be expected to increase cytotoxicity, these ruthenium-arene complexes are either equivalent or less cytotoxic than their nonfunctionalized analogues. Their antiproliferative activity follows the sequence **3b**$^+$ ≈ **3b** > **2b** > **1c** > **1b** > **4b**$^+$ > **5**$^+$ ≈ **4c**$^+$. Conversely, the antiproliferative activity toward the nontumorigenic HBL-100 cell line of compounds **1**−**5** tends to be higher than that of the previously studied RAPTA compounds, indicating an overall decrease in selectivity toward tumors and also suggesting that the general toxicity of the functionalized RAPTA compounds might be higher than that of RAPTA-C and RAPTA-B.

Drug uptake was determined by atomic absorption spectroscopy following exposure of the TS/A cells to 100 μM of the appropriate ruthenium-arene compound for 24 h, and the results from these studies are collected in Table 2.

The in vitro uptake study shows that the concentration of ruthenium in the treated cells is in the range 0.81×10^{-4} to 2.02×10^{-4} M and does not appear to strongly correlate with the corresponding IC_{50} value. Compared to the nonfunctionalized RAPTA compounds, intracellular uptake is somewhat lower, indicating that the functional group inhibits uptake. The ruthenium(II)-arene compounds may enter the tumor cells either by passive diffusion or by active transport, or even by a combination of these two processes, and since the uptake values are not too dissimilar between the charged and the neutral compounds, then active transport seems to be the preferred mechanism.

Oligomer Binding Studies and Computer Rationalization. The mode of activity of most metal-based drugs is believed to be via DNA binding, and organometallic compounds are no exception, having been known for many years to interact with DNA bases.[31] The DNA/oligomer binding of related ruthenium-arene compounds has already been extensively studied.[18,32] The activity of these new complexes with a 14-mer, 5′-ATACATG-GTACATA-3′, was investigated following the same procedure described for the previously reported RAPTA (and osmium analogues, OsAPTA) compounds.[32,33] Accordingly, compounds **1**−**5**, RAPTA-C, RAPTA-B, and RAPTA-T were incubated with the 14-mer at 37 °C for 72 h in a 1:1 and 2:1 (RAPTA:14-mer) ratio and the products analyzed by ESI-MS (see Figure 2 for a characteristic spectrum). The order of activity is **1b** ≈ **3b**$^+$ ≈ **3b** > **2b** ≈ **5**$^+$ ≈ **1c** ≈ RAPTA-C ≈ RAPTA-T > **4b**$^+$ ≈ **4c**$^+$ ≈ RAPTA-B. Full details of the products identified by ESI-MS are provided in the Supporting Information, and in Table 3 the ratio of total reacted versus unreacted 14-mer is given: essentially, the higher the value, the greater the reactivity of the compound toward the oligonucleotide. It is worth noting that the results are relative and the absolute product distribution depends on the purification procedure and mass spectrometer operating conditions, and caution must be applied when considering what actually occurs inside a cell. However, in keeping with our earlier study, two main types of adducts are formed, those with a "Ru(arene)PTA" unit bound to the 14-mer and those with a "RuPTA" unit, i.e., having lost the arene, as well as multiple binding. In contrast to RAPTA-C, RAPTA-B, and RAPTA-T, the adduct in which the arene is lost is the principal species for **1b**−**5**$^+$ and could be taken as a weakening of the ruthenium−arene bond due to the presence of electron-withdrawing substituents, and in order to test such a hypothesis, a DFT study has been undertaken (see below).

Density functional theory (DFT) calculations are a well-established tool used to describe the geometry and binding energies (BE) in transition metal complexes. In our previous work[32] we found that the calculated BEs for the metal−arene interaction change substantially upon modifications in RAPTA compounds (viz., nature of the arene, protonation or methylation of the PTA and the metal, i.e., Ru versus Os), whereas the metal−phosphine bond is only slightly affected. Here, the ruthenium−arene interaction was calculated for compounds **1b** and **3b** in vacuo and compared to the previously studied unfunctionalized arene compounds RAPTA-C and RAPTA-B.

(31) (a) Eisen, M. S.; Haskel, A.; Chen, H.; Olmstead, M. M.; Smith, D. P.; Maestre, M. F.; Fish, R. H. *Organometallics* **1995**, *14*, 2806. (b) Kuo, L. Y.; Kanatzidis, M. G.; Sabat, M.; Tipton, A. L.; Marks, T. J. *J. Am. Chem. Soc.* **1991**, *113*, 9027. (c) Smith, D. P.; Baralt, E.; Morales, B.; Olmstead, M. M.; Maestre, M. F.; Fish, R. H. *J. Am. Chem. Soc.* **1992**, *114*, 10647. (d) Smith, D. P.; Griffin, M. T.; Olmstead, M. M.; Maestre, M. F.; Fish, R. H. *Inorg. Chem.* **1993**, *32*, 4677. (e) Smith, D. P.; Kohen, E.; Maestre, M. F.; Fish, R. H. *Inorg. Chem.* **1993**, *32*, 4119. (f) Smith, D. P.; Olmstead, M. M.; Noll, B. C.; Maestre, M. F.; Fish, R. H. *Organometallics* **1993**, *12*, 593.

(32) Dorcier, A.; Dyson, P. J.; Gossens, C.; Rothlisberger, U.; Scopelliti, R.; Tavernelli, I. *Organometallics* **2005**, *24* (9), 2114.

(33) Morris, R. E.; Aird, R. E.; Murdoch, P. d. S.; Chen, H.; Cummings, J.; Hughes, N. D.; Parsons, S.; Parkin, A.; Boyd, G.; Jodrell, D. I.; Sadler, P. J. *J. Med. Chem.* **2001**, *44* (22), 3616.

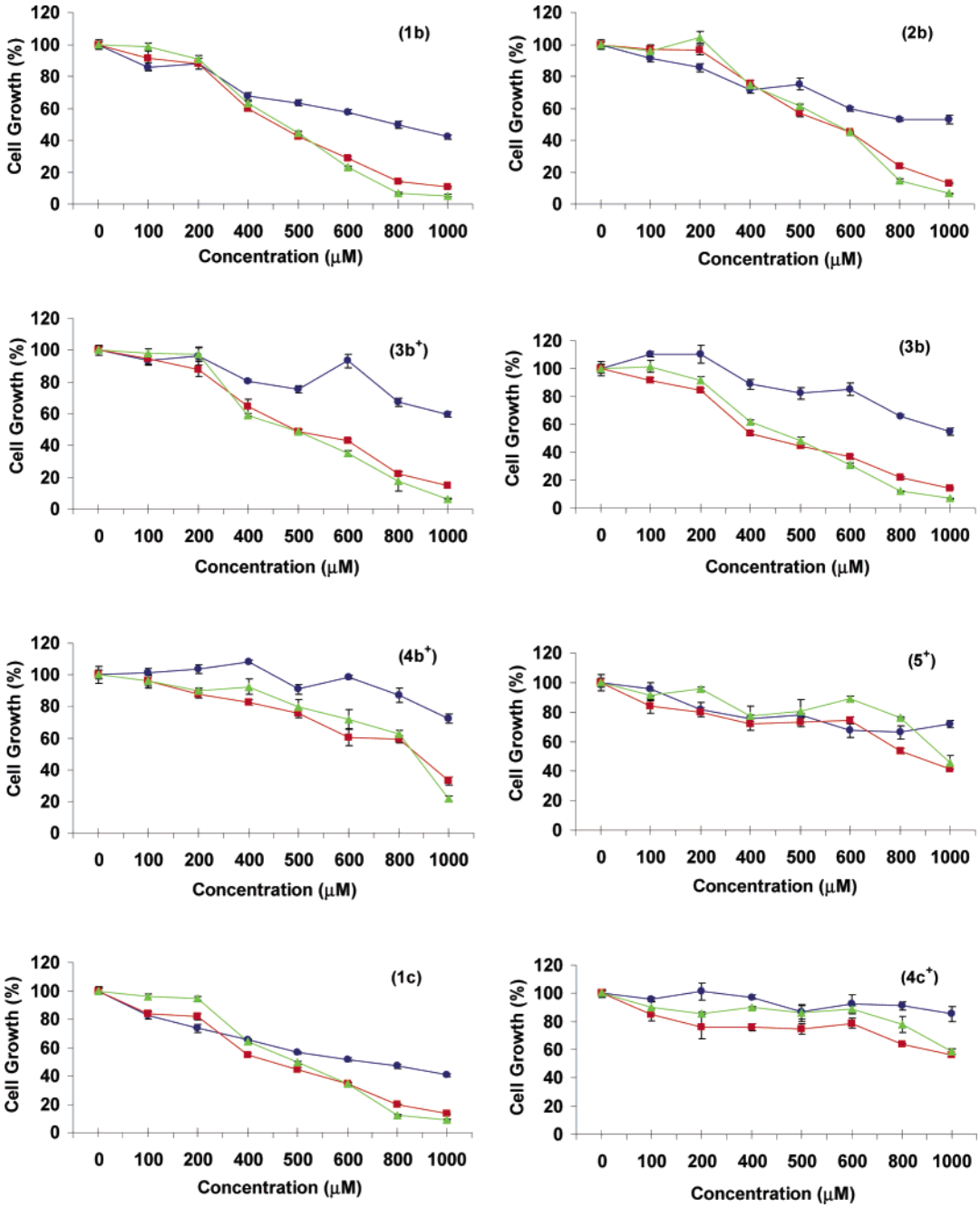

Figure 1. Effect of **1**−**5** on TS/A cell proliferation. The cells were sown on day 0 and treated on day 1 with a concentration range between 1 and 1000 μM of compound dissolved in the appropriate culture medium. The cell number was evaluated using the MTT test at the end of the treatment (● 24 h, ■ 48 h, and ▲ 72 h).

The ruthenium−arene binding energies were found to be very close in value, viz., 19.1 kcal/mol for **1b**, 20.4 kcal/mol for **3b**, 21.2 kcal/mol for RAPTA-C, and 19.5 kcal/mol for RAPTA-B. Furthermore, the potential energy surface (PES) that describes the rotation of the arene was found to be quite flat. In the case of compound **3b** different local minima were identified that differ by only ∼1 kcal/mol. More significantly, energy changes (ca. 10 kcal/mol and more) were observed between local minima representing different conformations of the aliphatic side chain of the arenes. Intramolecular H-bonds between these side chains and the PTA ligand were not observed. The bond distances and angles for all ligands (chloride, PTA, and arene) of **1b** and **3b** are almost identical to those of unfunctionalized arene compounds (see Table 4).

A detailed analysis of the electronic structure of **1b** and **3b** showed them to be again very similar (Table 5, Figures 3 and 4). However a difference was calculated for the dipole moment, which turns out to be slightly lower for the functionalized compounds **1b** and **3b**.

The HOMO is mainly localized on the ruthenium and chloride centers (bonding d−p-orbital interaction), with little bonding contribution between the arene π-orbitals and the ruthenium d-orbitals and no contributions from the PTA or from the functionalized arene side chain.

The LUMO is exclusively antibonding and is localized on the ruthenium (d-orbitals perpendicular to arene plane), the chlorides, and the arene, but not on the PTA and the functionalized arene side chain. In **1b**, **3b**, RAPTA-B, and RAPTA-C the calculated difference is not sufficiently large to explain the experimental results from the oligonucleotide binding study; thus other factors must dominate. The computational results suggest that the experimentally observed facilitated loss of arene is not

Table 1. IC_{50} Values of 1−5 on the TS/A and HBL-100 Cell Lines after 72 h Incubation Together with Other RAPTA Compounds for Comparison Purposes

compound	IC_{50}(TS/A) [μM]	IC_{50}(HBL-100) [μM]	(IC_{50}(HBL − 100))/(IC_{50}(TS/A))
1b	570	778	1.36
1c	538	715	1.33
2b	505	891	1.76
3b	458	813	1.78
3b$^+$	449	603	1.34
4b$^+$	820	666	0.81
4c$^+$	>1000	>1000	
5$^+$	>1000	612	<0.61
RAPTA-C[a]	507	>1000	>1.97
RAPTA-B[a]	231	>1000	>4.33
RAPTA-T[a]	74	>1000	>13.51

[a] RAPTA-C = $RuCl_2(\eta^6$-*p*-cymene)(PTA), RAPTA-B = $RuCl_2(\eta^6$-benzene)(PTA), RAPTA-T = $RuCl_2(\eta^6$-toluene)(PTA); data taken from ref 23.

Table 2. Ruthenium Uptake after Treatment for 24 h in TS/A Cells with 100 μM 1−5 and Other RAPTA Compounds for Comparison Purposes

compound	intracellular uptake (μg/10^6 cells)	intracellular uptake ($\times 10^{-4}$ M)
1b	0.06 ± 0.01	1.33 ± 0.20
1c	0.07 ± 0.006	1.39 ± 0.12
2b	0.07 ± 0.01	1.46 ± 0.30
3b	0.04 ± 0.004	0.95 ± 0.09
3b$^+$	0.10 ± 0.02	2.02 ± 0.38
4b$^+$	0.05 ± 0.005	1.05 ± 0.09
4c$^+$	0.05 ± 0.01	0.81 ± 0.19
5$^+$	0.06 ± 0.01	1.14 ± 0.21
RAPTA-C[b]	0.12 ± 0.02	2.55 ± 0.06
RAPTA-B[b]	0.13 ± 0.02	3.26 ± 0.04
RAPTA-T[b]	0.16 ± 0.02	2.9 ± 0.3

[a] Each number is the mean ± SE of an experiment done in triplicate. [b] RAPTA-C = $RuCl_2(\eta^6$-*p*-cymene)(PTA), RAPTA-B = $RuCl_2(\eta^6$-benzene)(PTA), RAPTA-T = $RuCl_2(\eta^6$-toluene)(PTA); data taken from ref 23.

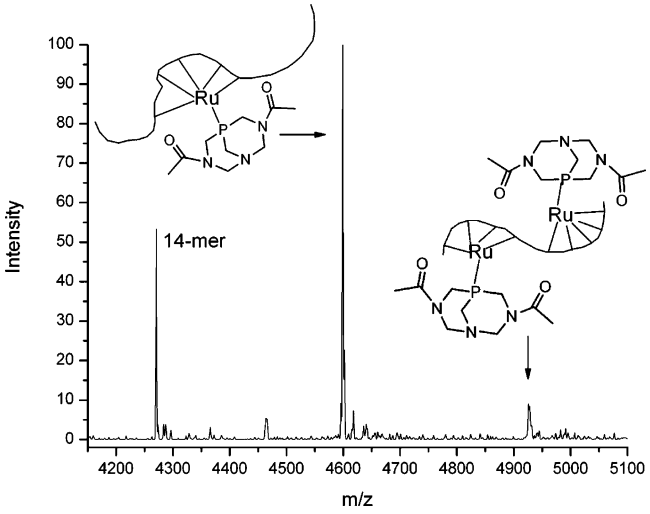

Figure 2. Negative ion ESI mass spectrum (deconvoluted using Max Ent software; see Experimental Section) of **1c** + 14-mer (2:1) in water (37 °C, 72 h incubation).

due to a thermodynamically weakened ruthenium−arene interaction induced by the functionalized arene, but is more likely due to kinetic or environmental effects. The frontier orbitals for the dichloride species are exclusively localized on the ruthenium, chloride, and η^6-arene centers, which suggests these are most reactive, and indeed, the chloride and arene ligands are lost on binding to the oligonucleotide.[32]

On the basis of a NMR structural assignment, the chelating species, **5**$^+$, was modeled prior to the X-ray experiment. Its calculated structure differs by only 0.114 Å/atom (RMSD on heavy atoms) and by just 0.036 Å (rmsd of the chelating arene ligand atoms) from its experimental counterpart. The atom C7 in the DFT structure is calculated to have an out of plane displacement of 0.529 Å (X-ray 0.526 Å, see below) from the plane spanned by the arene ring, C2−C6. Whereas the HOMO is significantly different (mainly localized on PTA and ruthenium) from those of the dichloride species, the LUMOs are very similar in both cases.

Table 3. Ratio of Reacted versus Unreacted 14-mer for 1−5 and Other RAPTA Compounds for Comparison Purposes[a]

	ratio reacted vs unreacted (RAPTA:14-mer 1:1)	ratio reacted vs unreacted (RAPTA:14-mer 2:1)
1b	0.40	10.57
1c	0.12	2.19
2b	0.20	2.61
3b	1.86	8.33
3b$^+$	0.95	4.75
4b$^+$	0	0.42
4c$^+$	0.05	0.33
5$^+$	0.05	1.69
RAPTA-C	0.20	2.62
RAPTA-B	0	0.35
RAPTA-T	0.10	0.83

[a] RAPTA-C = $RuCl_2(\eta^6$-*p*-cymene)(PTA), RAPTA-B = $RuCl_2(\eta^6$-benzene)(PTA), RAPTA-T = $RuCl_2(\eta^6$-toluene)(PTA).

Subsequently, the structure of **5**$^+$ was established by single-crystal X-ray diffraction analysis revealing a coordination sphere around the ruthenium with bonding parameters that are in excellent agreement with the calculated structure and not too different from other related ruthenium(II) arene complexes.[37] The structure of **5**$^+$ is shown in Figure 6, and selected bond lengths and angles are provided in Table 6 and compared to those of the calculated structure. The η^6-bound arene is slightly tilted, as can be seen from the somewhat longer distances from the metal to carbon atoms C(3), C(4), and C(5). Due to chelation of the arene ring via the amine moiety, carbon atom C(7) is markedly [0.53(1) Å] and carbon atom C(1) slightly [0.072(8) Å] out of the plane spanned by arene atoms C(2)−C(6). The crystal contains a water molecule that interacts via strong hydrogen bonding with the tetrafluoroborate anion, the NH_2 moiety, and the PTA ligand of a symmetry-related molecule [O(1)···F(3) 2.779(6) Å, O(1)···N(1) 2.966(6) Å, O(1)···N(3)* 2.841(6)]. As a consequence, the B(1)−F(3) bond, 1.416(9) Å, is slightly elongated relative to the other boron−fluorine bonds, 1.377(8)−1.386(8) Å. Further, a medium strong hydrogen bond stems from contacts of a nitrogen-proton to a fluorine atom of a symmetry-related BF_4 anion, N(1)···F(4) 3.077(7) Å.

Concluding Remarks

While it has been previously shown that the presence of substituent groups on the aromatic rings in titanocene-type drugs can potentially hydrogen bond to DNA, markedly increasing their cytotoxicity,[29] it is interesting to note that the addition of hydrogen-bonding substituents to the arene ligand in the RAPTA compounds does not enhance their cytotoxicity toward the cancer cell line screened, but actually has the reverse effect,

(34) Daigle, D. J.; Pepperman, A. B.; Vail, S. L. *J. Heterocycl. Chem.* **1974**, *11*, 407.
(35) Darensbourg, D.; Ortiz, C. G.; Kamplain, J. W. *Organometallics* **2004**, *23*, 1747.
(36) Onishi, T.; Miyaki, Y.; Asano, H.; Kurosawa, H. *Chem. Lett.* **1999**, *28*, 809.
(37) Miyaki, Y.; Onishi, T.; Kurosawa, H. *Inorg. Chim. Acta* **2000**, *300*−*302*, 369.

Table 4. Selected Calculated Angles (deg) and Distances (Å)

	M−Cl1	M−Cl2	M−P	M−η^6 [a]	P−M−Cl2	P−M−Cl1	Cl2−M−Cl1
1b	2.44	2.43	2.33	1.76	82.4	83.4	90.1
3b	2.44	2.44	2.32	1.76	82.9	82.9	90.8
RAPTA-B	2.44	2.44	2.33	1.75	82.6	82.6	90.9
RAPTA-C	2.44	2.44	2.33	1.76	82.3	83.8	89.9

[a] Distance between metal and center of aromatic ring.

Table 5. Selected Calculated Electronic Properties (dipoles in debye)

	Ru^{n+} [a]	dipole
1b	0.4923	6.445
3b	0.4805	6.948
RAPTA-B	0.4189	7.409
RAPTA-C	0.5114	7.486

[a] Mulliken charge on the ruthenium atom.

reducing cytotoxicity. In contrast, the cytotoxicity of RAPTA compounds with functionalized arenes toward the nontumorigenic cell line was increased. It is therefore not unreasonable to predict that the overall envisaged effect of such a modification on in vivo activity will correspond to a drug that is not only less active, but will have a greater general toxicity, leading to more unwanted side-effects.

The origins of the effects on the in vitro cell studies are not easily traced. There is a modest correlation between the IC_{50} values of the compounds and drug uptake, but not with respect to the reactivity with the oligonucleotide (as estimated by ESI-MS), as can be seen from Figure 7: there is no correlation between IC_{50} and the reactivity with the oligonucleotide.

From Figure 7 it is clear that the IC_{50} values for the functionalized compounds that are naturally charged, viz., **4b**$^+$, **4c**$^+$, and **5**$^+$ (but not **3b**$^+$), show the least activity and that for these compounds drug uptake is also the lowest. These compounds are also among the least reactive toward the oligonucleotide in terms of total reactivity, but the most reactive with respect to the loss of the arene (see Supporting Information). While it is not possible to speculate as to whether loss of the arene occurs in vitro (or in vivo), we were able to show using DFT calculations that arene loss is not correlated to the strength of the ruthenium−arene bond. It is not unreasonable to assume that loss of the arene is connected to the solubility of the arene in aqueous media, the most hydrophobic arenes preferring to remain bound to the ruthenium-PTA unit and the most hydrophilic dissociating more readily. The higher hydrophilicity of the functionalized arene RAPTA compounds, relative to RAPTA-C, RAPTA-B, and RAPTA-T, is also probably responsible for the reduced uptake in the cells. Finally, while DNA binding cannot be ruled out as the principal mechanism for the cytotoxicity of the RAPTA compounds, other potential targets clearly need to be investigated.

Experimental Section

Synthesis and Chemical Characterization. The starting materials 1,3,5-triaza-7-phosphaadamantane (PTA),[34] 3,7-diacetyl-1,3,7-triaza-5-phosphabicyclo[3.3.1]nonane (DAPTA),[35] **1a**,[36] and **4a**[37] were prepared as described previously. All commercially available reagents were used without further purification, unless specified. Reactions were carried out under a nitrogen atmosphere, and solvents were purged with nitrogen before use. ^{1}H, ^{13}C, and ^{31}P NMR spectra were recorded on a Bruker 400 MHz Ultrashield spectrometer. Electrospray ionization mass spectra (ESI-MS) were obtained on a Thermofinigan LCQ Deca XP Plus quadrupole ion trap instrument set in positive mode using a literature method.[38]

$RuCl_2(\eta^6$-$C_6H_5(CH_2)_2OH)$(PTA), 1b. To a suspension of **1a** (1.02 g, 1.70 mmol) in MeOH/CH_2Cl_2 (1:1, 60 mL) was added PTA (620 mg, 4.0 mmol), and the resulting mixture was stirred for 30 min at 50 °C. The resulting dark red solution was filtered, the solvent was removed in vacuo, and the remaining solid was washed with diethyl ether to afford the product as an orange powder. Yield: 1.48 g (96%).

^{1}H NMR (d_6-DMSO, 400 MHz): 5.77 (dd, 2H, H^{3,5}), 5.63 (d, $^3J_{HH}$ = 5.8, 2H, H^{2,6}), 5.33 (t, $^3J_{HH}$ = 5.3, 1H, H^4), 4.73 (t, $^3J_{HH}$ = 5.0, 1H, O*H*), 4.43, (br, 6H, H^{15}), 4.19 (br, 6H, H^{14}), 3.66 (dt, $^3J_{HH}$ = 5.0, $^3J_{HH}$ = 6.2, 2H, H^8), 2.42 (t, $^3J_{HH}$ = 6.2, 2H, H^7). ^{13}C NMR (d_6-DMSO, 100 MHz): 106.6 (d, $^2J_{CP}$ = 4, C^1), 88.0 (d, $^2J_{CP}$ = 5, C^{2,6}), 86.2 (d, $^2J_{CP}$ = 2, C^{3,5}), 78.5 (C^4), 72.7 (d, $^3J_{CP}$ = 7, C^{15}), 60.5 (C^8), 52.3 (d, $^1J_{CP}$ = 17, C^{14}), 36.5 (C^7). ^{31}P NMR (d_6-DMSO, 162 MHz): −31.9 (s). ESI-MS (H_2O): *m*/*z* = 416.0 [$RuCl(\eta^6$-$C_6H_5(CH_2)_2OH)(PTA)]^+$. Anal. Calcd for $C_{14}H_{22}Cl_2N_3OPRu\cdot 1/2\,H_2O$: C, 35.83; H, 5.15; N, 8.95. Found: C, 36.01; H, 5.00; N, 8.95.

$RuCl_2(\eta^6$-$C_6H_5(CH_2)_2OH)$(DAPTA), 1c. To a suspension of **1a** (51 mg, 0.087 mmol) in MeOH/CH_2Cl_2 (1:1, 12 mL) was added DAPTA (43 mg, 0.175 mmol), and the mixture stirred at room temperature for 2 h. The solution was then concentrated and diethyl ether added in order to precipitate the product, which was then isolated and washed with diethyl ether. Yield: 80 mg (89%).

^{1}H NMR (d_6-DMSO, 400 MHz): 5.90 (br, 2H, H^{3,5}), 5.74 (br, H^{2,6}), 5.55 (d, $^1J_{HH}$ = 14.0, 1H, H^{15}), 5.49 (br, 1H, H^4), 5.28 (dd, $^1J_{HH}$ = 14.9, $^2J_{PH}$ = 7.9, 1H, H^{16}), 4.97 (d, $^1J_{HH}$ = 14.0, 1H, H^{17}), 4.77 (br, 1H, O*H*), 4.66 (d, $^1J_{HH}$ = 14.0, 1H, H^{17}), 4.48 (dd, $^1J_{HH}$ = 14.9, $^2J_{PH}$ = 9.3, 1H, H^{14}), 4.20 (d, $^1J_{HH}$ = 14.9, 1H, H^{14}), 4.13 (d, $^1J_{HH}$ = 14.0, 1H, H^{15}), 4.04 (d, $^1J_{HH}$ = 14.9, 1H, H^{18}), 3.95 (d, $^1J_{HH}$ = 14.9, 1H, H^{18}), 3.69 (br, 3H, H,^{8}H^{16}), 2.46 (br, 2H, H^7), 1.97 (s, 3H, H^{20}), 1.90 (s, 3H, H^{22}). ^{13}C NMR (d_6-DMSO, 100 MHz): 169.5 (C^{21}), 168.9 (C^{19}), 108.2 (d, $^2J_{CP}$ = 4, C^1), 88.5 (d, $^2J_{CP}$ = 6, C$^{2/6}$), 88.2 (d, $^2J_{CP}$ = 5, C$^{2/6}$), 87.1 (d, $^2J_{CP}$ = 1, C$^{3/5}$), 87.0 (d, $^2J_{CP}$ = 1, C$^{3/5}$), 79.0 (C^4), 67.1 (d, $^3J_{CP}$ = 5, C^{17}), 61.6 (d, $^3J_{CP}$ = 4, C^{15}), 60.4 (C^8), 49.1 (d, $^1J_{CP}$ = 23, C^{18}), 43.9 (d, $^1J_{CP}$ = 23, C^{14}), 39.3 (d, $^1J_{CP}$ = 22, C^{16}), 36.6 (C^7), 21.9 (C^{22}), 21.8 (C^{20}). ^{31}P NMR (d_6-DMSO, 162 MHz): −11.8 (s). ESI-MS (H_2O): *m*/*z* = 488.0 [$RuCl(\eta^6$-$C_6H_5(CH_2)_2OH)$(DAPTA)]$^+$. Anal. Calcd for $C_{17}H_{26}Cl_2N_3O_3PRu\cdot H_2O$: C, 37.72; H, 5.21; N, 7.76. Found: C, 37.68; H, 4.89; N, 7.26.

$[RuCl_2(\eta^6$-$C_6H_5(CH_2)_2CH(OH)CH_3)]_2$, 2a. To a solution of $RuCl_3\cdot 3H_2O$ (2.34 g, 8.95 mmol) in ethanol (70 mL) was added 4-(cyclohexa-1,4-dienyl)butan-2-ol (3.95 g, 26.78 mmol), and the solution refluxed for 8 h, during which time an orange precipitate forms. The mixture was filtered and the remaining solid washed with ethanol (15 mL) and diethyl ether (15 mL) to afford **2a**. Yield: 2.65 g (92%).

^{1}H NMR (d_6-DMSO, 400 MHz): 5.98 (m, 4H), 5.73 (m, 6H), 3.63 (m, 2H, H^9), 2.51 (m, 4H, H^7), 1.62 (m, 4H, H^8), 1.08 ($^3J_{HH}$ = 6.1, 6H, H^{10}). ^{13}C NMR (d_6-DMSO, 100 MHz): 108.9 (C^1), 89.5/89.4 (C^{2,6}), 85.3/85.2 (C^{3,5}), 83.3 (C^4), 65.8 (C^9), 39.0 (C^8), 29.9 (C^7), 24.2 (C^{10}).

$RuCl_2(\eta^6$-$C_6H_5(CH_2)_2CH(OH)CH_3)$(PTA), 2b. To a suspension of $[RuCl_2(\eta^6$-$C_6H_5(CH_2)_2CH(OH)CH_3)]_2$ (**2a**) (1.00 g, 1.55 mmol) in a mixture of MeOH/CH_2Cl_2 (1:1, 60 mL) was added PTA (560 mg, 3.4 mmol), and the mixture was stirred at room temperature

(38) Dyson, P. J.; McIndoe, J. S. *Inorg. Chim. Acta*. **2003**, *354*, 68.

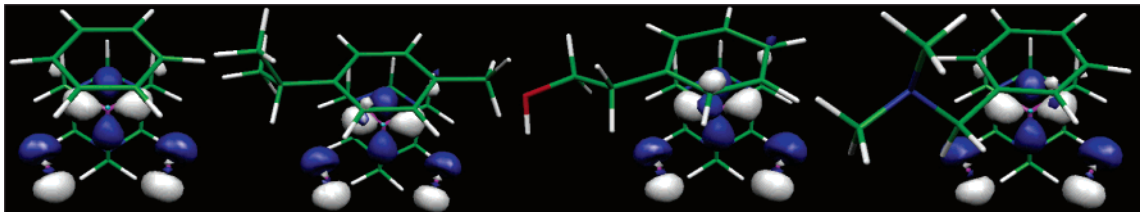

Figure 3. HOMO (contour at 0.07); from left to right: RAPTA-B, RAPTA-C, **1b**, and **3b**.

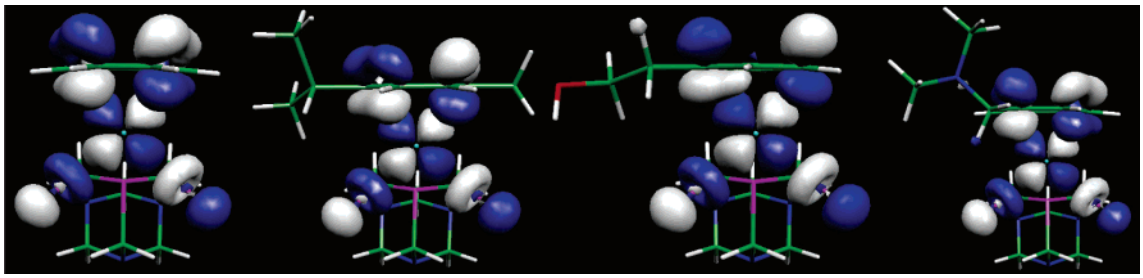

Figure 4. LUMO (contour at 0.04); from left to right: RAPTA-B, RAPTA-C, **1b**, and **3b**.

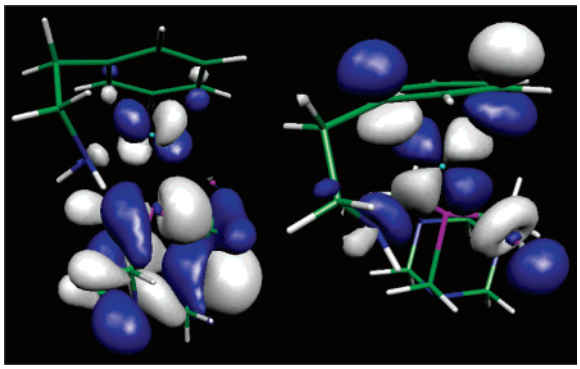

Figure 5. HOMO (left; contour at 0.025) and LUMO (right; contour at 0.04) of $\mathbf{5}^+$.

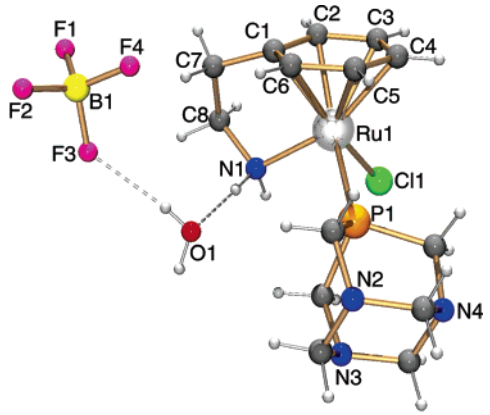

Figure 6. Ball-and-stick representation of $\mathbf{5}^+$.

for 4 h. The solution was filtered, the solvents were evaporated in vacuo, and the remaining solid was recrystallized from $CHCl_3/Et_2O$ to afford the product as an orange powder. Yield: 1.40 g (94%).

^{1}H NMR (d_6-DMSO, 400 MHz): 5.78 (br, 2H, $H^{3,5}$), 5.60 (d, $^3J_{HH}$ = 5.9, 1H, $H^{2/6}$), 5.56 (d, $^3J_{HH}$ = 6.1, 1H, $H^{2/6}$), 5.30 (dd, 1H, H^4), 4.45 ($^3J_{HH}$ = 5.0, 1H, O*H*), 4.43 (s, 6H, H^{15}), 4.18 (s, 6H, H^{14}), 3.61 (m, H^9), 2.34 (m, 2H, H^7), 1.59 (m, 2H, H^8), 1.07 ($^3J_{HH}$ = 6.4, 3H, H^{10}). ^{13}C NMR (d_6-DMSO, 100 MHz): 109.9 (d, $^2J_{CP}$ = 4, C^1), 87.1 (d, $^2J_{CP}$ = 6, $C^{2/6}$), 86.8 (d, $^2J_{CP}$ = 6, $C^{2/6}$), 86.5 ($C^{3,5}$), 77.9 (C^4), 72.7 (d, $^2J_{CP}$ = 7, C^{15}), 65.8 (C^9), 52.3 (d, $^2J_{CP}$ = 17, C^{14}), 39.0 (C^8), 29.6 (C^7), 24.1 (C^{10}). ^{31}P NMR (d_6-DMSO, 162 MHz): −31.9 (s). ESI-MS (H_2O): m/z = 479.9 [$RuCl_2(\eta^6$-$C_6H_5(CH_2)_2CH(OH)CH_3)(PTA)+H]^+$, 444.0 [$RuCl(\eta^6$-$C_6H_5(CH_2)_2$-$CH(OH)CH_3)(PTA)]^+$, 408.1 [$Ru(\eta^6$-$C_6H_5(CH_2)_2CH(OH)CH_3)$-$(PTA)]^+$. Anal. Calcd for $C_{16}H_{26}Cl_2N_3OPRu\cdot 1/2H_2O$: C, 39.35; H, 5.57; N, 8.60. Found: C, 39.34; H, 5.55; N, 8.64.

Table 6. Selected Bond Lengths (Å) and Angles (deg) of $\mathbf{5}^+$ Obtained from DFT Calculations and X-ray Diffraction Analysis

	calculated	X-ray
Ru−C1	2.176	2.159(5)
Ru−C2	2.272	2.154(5)
Ru−C3	2.281	2.253(6)
Ru−C4	2.283	2.233(6)
Ru−C5	2.257	2.203(7)
Ru−C6	2.245	2.192(6)
Ru−N	2.172	2.127(5)
Ru−Cl	2.412	2.417(2)
Ru−P	2.360	2.324(1)
C1−C7−C8	108.9	108.6(5)
Cl−Ru−P	82.8	84.43(5)
Cl−Ru−N	83.9	85.9(1)
N−Ru−P	93.0	90.1(1)

$[(RuCl_2(\eta^6$-$C_6H_5CH_2N(CH_3)_2H)_2]Cl_2$, 3a. To a solution of $RuCl_3\cdot 3H_2O$ (2.06 g, 7.88 mmol) in ethanol (70 mL) was added (cyclohexa-1,4-dienyl)-*N*,*N*-dimethylmethanamine hydrochloride (4.10 g, 23.6 mmol), and the solution refluxed for 6 h, during which time an orange precipitate formed. The mixture was filtered and the remaining solid washed with ethanol (15 mL) and diethyl ether (15 mL) to afford **3a** as brown solid. Yield: 2.45 g (90%).

^{1}H NMR (d_6-DMSO, 400 MHz): 6.33 (d, $^3J_{HH}$ = 5.8, 4H, $H^{2,6}$), 6.14 (m, 4H, $H^{3,5}$), 6.10 (m, 2H, H^4), 4.05 (s, 4H, H^7), 2.80 (s, 6H, $H^{8,9}$). ^{13}C NMR (d_6-DMSO, 100 MHz): 92.6 ($C^{2,6}$), 89.3 (C^4), 88.7 (C^1), 86.7 ($C^{3,5}$), 58.1 (C^7), 42.3 ($C^{9,10}$).

$[RuCl_2(\eta^6$-$C_6H_5CH_2N(CH_3)_2H)(PTA)]Cl$, 3b$^+$. To a suspension of $[(RuCl_2(\eta^6$-$C_6H_5CH_2N(CH_3)_2H)_2]Cl_2$ (**3a**) (1.02 g, 1.45 mmol) in a mixture of $MeOH/CH_2Cl_2$ (1:1, 200 mL) was added PTA (460 mg, 2.90 mmol), and the obtained solution was stirred at room temperature for 30 min. The resulting solution was filtered, the solvent removed in vacuo, and the remaining solid recrystallized from hot methanol to afford the product as an orange powder. Yield: 1.07 g (74%).

^{1}H NMR (d_6-DMSO, 400 MHz): 6.07 (d, $^3J_{HH}$ = 5.5, 2H, $H^{2,6}$), 5.93 (dd, $^3J_{HH}$ = 5.5, $^3J_{HH}$ = 4.9, 2H, $H^{3,5}$), 5.64 (t, $^3J_{HH}$ = 4.9, 1H, H^4), 4.47 (br, 6H, H^{15}), 4.23 (br, 6H, H^{14}), 3.83 (s, H^7), 2.73 (s, $H^{8,9}$). ^{13}C NMR (d_6-DMSO, 100 MHz): 103.2 (d, $^2J_{CP}$ = 6, C^1), 92.1 (br, $C^{2,6}$), 85.2 (d, $^2J_{CP}$ = 2, $C^{3,5}$), 82.4 (br, C^4) 72.5 (d, $^3J_{CP}$ = 7, C^{15}), 58.7 (C^7), 52.2 (d, $^1J_{CP}$ = 18, C^{14}), 42.0 ($C^{9,10}$). ^{31}P NMR (d_6-DMSO, 162 MHz): −30.6 (s). ESI-MS (H_2O): m/z = 464.9 [$RuCl_2(\eta^6$-$C_6H_5CH_2N(CH_3)_2H)(PTA)]^+$. Anal. Calcd for

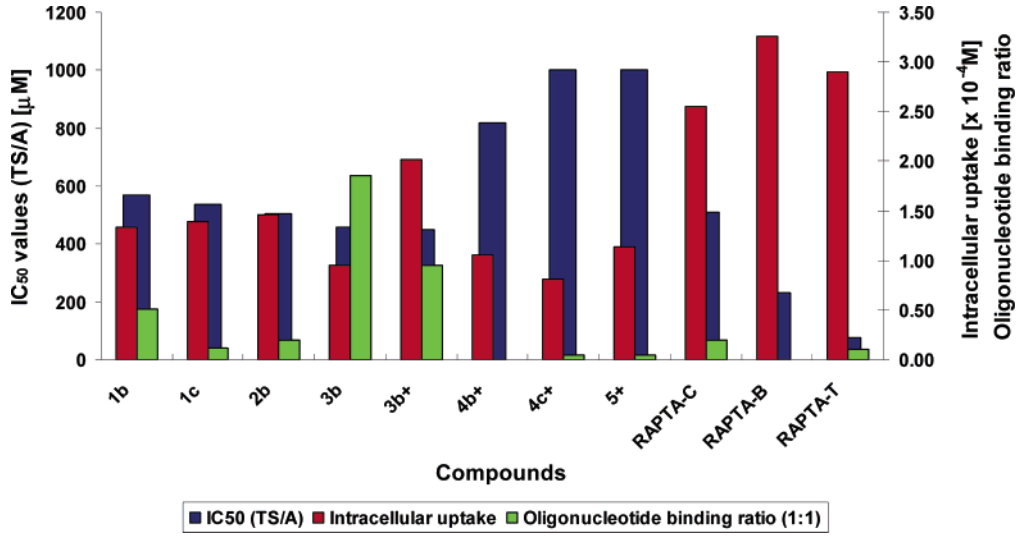

Figure 7. Graph comparing IC_{50}, drug uptake, and relative reactivity toward reactions with the oligonucleotide.

$C_{15}H_{26}Cl_3N_4PRu\cdot 2H_2O$: C, 33.6; H, 5.6; N, 10.4. Found: C, 33.0; H, 5.1; N, 10.4.

$RuCl_2(\eta^6\text{-}C_6H_5CH_2N(CH_3)_2)$(PTA), 3b. Complex **3b**$^+$ (832 mg, 1.70 mmol) was dissolved in methanol (100 mL), a solution of KOH (100 mg, 1.85 mmol) in methanol was added, and the mixture was stirred for 15 min at RT. The solvent was removed and the residue extracted with $CHCl_3$ to afford the product as an orange solid. Yield: 526 mg (48%).

^{1}H NMR (d_6-DMSO, 400 MHz): 5.77 (dd, $^3J_{HH}$ = 5.8, $^3J_{HH}$ = 5.3, 2H, H^{3,5}), 5.70 (d, $^3J_{HH}$ = 5.8, 2H, H^{2,6}), 5.44 (t, $^3J_{HH}$ = 5.3, 1H, H^4), 4.43 (br, 6H, H^{15}), 4.19 (br, 6H, H^{14}), 3.16 (s, 2H, H^7), 2.22 (s, 6H, H^{8,9}). ^{13}C NMR (d_6-DMSO, 100 MHz): 103.9 (C^1), 88.9 (d, $^2J_{CP}$ = 5, C^{2,6}), 85.5 (d, $^2J_{CP}$ = 2, C^{3,5}), 79.5 (C^4), 72.6 (d, $^3J_{CP}$ = 7, C^{15}), 60.4 (C^7), 52.4 (d, $^1J_{CP}$ = 18, C^{14}), 45.5 (C^{8,9}). ^{31}P NMR (d_6-DMSO, 162 MHz): −31.1 (s). ESI-MS (H_2O): m/z = 464.9 [$RuCl_2(\eta^6\text{-}C_6H_5CH_2N(CH_3)_2$)(PTA)+H]$^+$. Anal. Calcd for $C_{15}H_{25}Cl_2N_4PRu\cdot 2H_2O$: C, 36.0; H, 5.84; N, 11.20. Found: C, 36.22; H, 5.3; N, 11.2.

[$RuCl_2(\eta^6\text{-}C_6H_5(CH_2)_2NH_3$)(PTA)]Cl, 4b$^+$. To a suspension of **4a** (1.5 g, 2.28 mmol) in DMF (250 mL) was added PTA (720 mg, 4.58 mmol), and the mixture stirred at room temperature for 40 min. The resulting dark red solution was filtered, the solvent evaporated in vacuo, and the remaining solid washed with CH_2Cl_2 to afford the product as an orange powder. Yield: 1.40 g (63%).

^{1}H NMR (d_6-DMSO, 400 MHz): 8.18 (br, 3H, N*H*), 5.81 (br, H^{3,5}), 5.76 (br, H^{2,6}), 5.50 (br, H^4), 4.47 (m, 6H, H^{15}), 4.21 (s, 6H, H^{14}), 3.15 (br, 2H, H^8), 2.67 (br, 2H, H^7). ^{13}C NMR (d_6-DMSO, 100 MHz): 104.0 (d, $^2J_{CP}$ = 6, C^1), 88.9 (d, $^2J_{CP}$ = 5, C^{2,6}), 85.5 (C^{3,5}), 79.4 (C^4), 72.5 (d, $^3J_{CP}$ = 7, C^{15}), 52.2 (d, $^1J_{CP}$ = 17, C^{14}), 38.4 (C^8), 30.9 (C^7). ^{31}P NMR (d_6-DMSO, 162 MHz): −31.0 (s). ESI-MS (H_2O): m/z = 451.0 [$RuCl_2(\eta^6\text{-}C_6H_5(CH_2)_2NH_3$)(PTA)]$^+$. Anal. Calcd for $C_{14}H_{24}Cl_3N_4PRu\cdot 1/2H_2O$: C, 33.92; H, 5.08; N, 11.30. Found: C, 33.66; H, 5.07; N, 11.60.

[$RuCl_2(\eta^6\text{-}C_6H_5(CH_2)_2NH_3$)(DAPTA)]Cl, 4c$^+$. To a suspension of **4a** (150 mg, 0.23 mmol) in DMF (25 mL) was added DAPTA (105 mg, 0.46 mmol), and the mixture stirred for 1 h at room temperature. The resulting deep red solution was filtered and the solvent removed in vacuo. Diethyl ether was added to precipitate the product, which was isolated and washed with diethyl ether. Yield: 210 mg (82%).

^{1}H NMR (d_6-DMSO, 400 MHz): 8.17 (br, 3H, N*H*), 5.94 (br, 2H, H^{3,5}), 5.85 (br, H^{2,6}), 5.64 (br, 1H, H^4), 5.55 (d, $^1J_{HH}$ = 13.3, 1H, H^{15}), 5.28 (dd, $^1J_{HH}$ = 15.2, $^2J_{PH}$ = 7.6, 1H, H^{16}), 4.98 (d, $^1J_{HH}$ = 14.0, 1H, H^{17}), 4.71 (d, $^1J_{HH}$ = 14.0, 1H, H^{17}), 4.47 (dd, $^1J_{HH}$ = 15.2, $^2J_{PH}$ = 9.0, 1H, H^{14}), 4.23 (br, 1H, H^{14}), 4.16 (d, $^1J_{HH}$ = 13.3, 1H, H^{15}), 4.09 (d, $^1J_{HH}$ = 14.9, 1H, H^{18}), 3.99 (d, $^1J_{HH}$ = 14.9, 1H, H^{18}), 3.72 (br, 1H, H^{16}), 3.18 (br, 2H, H^8), 2.72 (t, $^3J_{HH}$ = 7.6, 2H, H^7), 1.97 (s, 3H, H^{20}), 1.90 (s, 3H, H^{22}). ^{13}C NMR (d_6-DMSO, 100 MHz): 169.4 (C^{21}), 168.9 (C^{19}), 105.4 (d, $^2J_{CP}$ = 6, C^1), 89.2 (d, $^2J_{CP}$ = 5, C$^{2/6}$), 89.1 (d, $^2J_{CP}$ = 5, C$^{2/6}$), 86.3 (br, C^{3,5}), 79.6 (C^4), 67.1 (d, $^3J_{CP}$ = 4, C^{17}), 61.6 (d, $^3J_{CP}$ = 5, C^{15}), 49.3 (d, $^1J_{CP}$ = 23, C^{18}), 43.9 (d, $^1J_{CP}$ = 23, C^{14}), 39.3 (d, $^1J_{CP}$ = 22, C^{16}), 38.3 (C^8), 30.9 (C^7), 21.9 (C^{22}), 21.8 (C^{20}). ^{31}P NMR (d_6-DMSO, 162 MHz): −11.7 (s). ESI-MS (H_2O): m/z = 522.9 [$RuCl_2(\eta^6\text{-}C_6H_5(CH_2)_2NH_3$)(DAPTA)]$^+$, m/z = 487.1 [$RuCl(\eta^6\text{-}C_6H_5(CH_2)_2NH_2$)(DAPTA)]$^+$. Anal. Calcd for $C_{17}H_{28}Cl_3N_4O_2PRu$: C, 36.54; H, 5.05; N, 10.03. Found: C, 36.29; H, 5.58; N, 10.36.

[$RuCl(\eta^6\text{-}C_6H_5(CH_2)_2NH_2$)(PTA)][$BF_4$], 5$^+$. To a suspension of **4b**$^+$ (300 mg, 0.62 mmol) in methanol (70 mL) was added a solution of NaOH (25 mg, 0.62 mmol) in methanol (2 mL), and the mixture was stirred for 15 min at room temperature. Then $AgBF_4$ (121 mg, 0.62 mmol) was added, and the solution was stirred overnight. The mixture was filtered, the solvent removed, and the remaining solid washed with diethyl ether to afford the product as a yellow powder. Yield: 201 mg (65%).

^{1}H NMR (d_6-DMSO, 400 MHz): 8.18 (br, 3H, N*H*), 5.81 (br, H^{3,5}), 5.76 (br, H^{2,6}), 5.50 (br, H^4), 4.47 (m, 6H, H^{15}), 4.21 (s, 6H, H^{14}), 3.15 (br, 2H, H^8), 2.67 (br, 2H, H^7). ^{13}C NMR (d_6-DMSO, 100 MHz): 104.0 (d, $^2J_{CP}$ = 6, C^1), 88.9 (d, $^2J_{CP}$ = 5, C^{2,6}), 85.5 (C^{3,5}), 79.4 (C^4), 72.5 (d, $^3J_{CP}$ = 7, C^{15}), 52.2 (d, $^1J_{CP}$ = 17, C^{14}), 38.4 (C^8), 30.9 (C^7). ^{31}P NMR (d_6-DMSO, 162 MHz): −33.6 (s). ESI-MS (H_2O): 415.0 [$RuCl(\eta^6\text{-}C_6H_5(CH_2)_2NH_2$)(PTA)]$^+$. Anal. Calcd for $C_{14}H_{23}BClF_4N_4PRu\cdot H_2O$: C, 32.36; H, 4.88; N, 10.78. Found: C, 32.25; H, 4.87; N, 10.78.

Crystallography. Crystals suitable for X-ray diffraction were obtained from slow diffusion of diethyl ether into a dichloromethane solution of **5**$^+$. Data collection for the X-ray structure determination was performed on a KUMA CCD diffractometer system by using graphite-monochromated Mo Kα (0.71070 Å) radiation and a low-temperature device (T = 140(2) K). Data reduction was performed by CrysAlis RED[39] and the structure solved and refined with SHELX97.[40] Graphical representation of the structure was made with ORTEP32.[41] The structure was solved by Patterson methods and successive interpretation of the difference Fourier maps, followed by full matrix least-squares refinement (against F^2). Atoms were refined anisotropically, and the contribution of the hydrogen atoms, in their calculated positions, was included in the refinement

(39) *CrysAlis RED*; Oxford Diffraction Ltd, M. P.: Abingdon, OX14 4 RX, UK, 2003.

(40) Sheldrick, G. M. *SHELX-97*, Structure Solution and Refinement Package; Universität Göttingen, 1997.

(41) Farrugia, L. J. *J. Appl. Crystallogr.* **1997**, *30*, 565.

Table 7. Crystallographic Data for 5^+

formula	$C_{14}H_{23}BClF_4N_4PRu \cdot H_2O$
M	519.68
T [K]	140(2)
crystal system	monoclinic
space group	$P2_1/n$
a [Å]	11.1961(10)
b [Å]	14.3501(13)
c [Å]	12.3751(11)
α [deg]	90.0
β [deg]	103.432(8)
γ [deg]	90.0
V [Å^3]	1933.9(3)
Z	4
density [Mg/m^3]	1.785
μ [mm^{-1}]	1.081
2θ range [deg]	$3.14 \leq 2\theta \leq 25.03$
no. of reflns collected	11045
no. of indep reflns	3288 [$R_{int} = 0.0696$]
goodness-of-fit on F^2	1.204
final R1, wR2 [$I > 2\sigma(I)$]	0.0484, 0.1150

using a riding model, with the exception of the water-hydrogen atoms, which were located on the Fourier map and constrained using the DFIX command. Relevant crystallographic data are compiled in Table 7.

In Vitro Tests. The TS/A murine adenocarcinoma cell line, initially obtained from Dr. G. Forni (CNR, Centro di Immunogenetica ed Oncologia Sperimentale, Torino, Italy), belongs to the tumor cell line panel of the Callerio Foundation and is stored in liquid nitrogen. Cells were cultured according to a standard procedure[42] and maintained in RPMI-1640 medium (EuroClone, Wetherby, U.K.) supplemented with 10% fetal bovine serum (FBS, Invitrogen, Milano, Italy), 2 mM L-glutamine (EuroClone, Wetherby, U.K.), and 50 μg/mL gentamycin sulfate solution (EuroClone, Wetherby, U.K.). The cell line was kept in an incubator with 5% CO_2 and 100% relative humidity at 37 °C. Cells from a confluent monolayer were removed from flasks by a trypsin-EDTA solution (EuroClone, Wetherby, U.K.).

HBL-100, nontumorigenic human breast cells, obtained from ATCC (American Type Culture Collection), were maintained in McCoy's 5A medium (Sigma, St. Louis, MO) supplemented with 10% FBS, 2 mM L-glutamine, 100 UI/mL penicillin, and 100 μg/mL streptomycin (EuroClone, Whetherby, UK), in a humidified atmosphere with 5% CO_2 at 37 °C.

Cell viability was determined by the trypan blue dye exclusion test. For experimental purposes, the cells were sown in multiwell cell culture plastic plates (Corning Costar Italia, Milano, Italy). Cell growth was determined by the MTT viability test.[43] Cells were sown on 96-well plates and after 24 h were incubated with the appropriate compound at a concentration of 1−1000 μM, prepared by dissolving in a medium containing 5% serum, for 24, 48, and 72 h. Analysis was performed at the end of the incubation time. Briefly, MTT [3-(4,5-dimethylthiazol-2-yl)-2,5-diphenyltetrazolium bromide] dissolved in PBS (5 mg/mL) was added (10 μL per 100 μL of medium) to all wells, and the plates were then incubated at 37 °C with 5% CO_2 and 100% relative humidity for 4 h. After this time, the medium was discarded and 100 μL of DMSO (Sigma, St. Louis, MO) was added to each well according to the method of Alley et al.[44] Optical density was measured at 570 nm on a Packard SpectraCount (Meriden, CT) instrument.

Determination of Intracellular Ruthenium. Ruthenium cell uptake was determined by atomic absorption spectroscopy (AAS) on samples processed using the procedure of Tamura and Arai with slight modifications.[45] For each complex tested, a six-well plate was prepared by seeding 125 000 TS/A cells in 3 mL of complete medium with 5% FBS to each experimental and control well. The plate was incubated for 24 h at 37 °C. Control wells are filled with 3 mL of complete medium and experimental wells with 3 mL of a 100 μM solution of RAPTA compounds prepared in complete medium. The plate was incubated for 24 h at 37 °C and washed three times with PBS before the cells were collected and counted with the trypan blue exclusion test, and the intracellular concentration of ruthenium was determined. After this treatment, the cells were dried in Nalgene cryogenic vials (a first drying step was performed overnight at 80 °C and a second step at 105 °C until the samples reached a constant weight). The dried cells were decomposed by the addition of an aliquot of tetramethylammonium hydroxide (25% in water) (Aldrich Chimica, Gallarate, Milano, Italy) and of milliQ water at a ratio of 1:1 directly in each vial, at room temperature and under shaking. Final volumes were adjusted to 1 mL with milliQ water. The concentration of ruthenium in the TS/A tumor cell line was measured in triplicate by flameless atomic absorption spectroscopy (AAS) using a Zeeman graphite tube atomizer, model SpectrAA-300, supplied with a specific ruthenium emission lamp (hollow cathode lamp P/N 56-101447-00; Varian, Mulgrave, Victoria, Australia). Quantification of ruthenium was carried out in 10 μL samples at 349.9 nm with an atomizing temperature of 2500 °C, using argon as carrier gas at a flow rate of 3.0 L/min (for further details concerning the furnace parameter settings, see ref 46). Before each analysis, a five-point calibration curve was obtained to check the range of linearity using a ruthenium custom-grade standard, 998 mg/mL (Inorganic Ventures, Lakewood, NJ).

Oligonucleotide Binding. The 14-mer oligonulcleotide (5′-ATACATGGRACATA-3′) was obtained from MWG Biotech AG (Ebersberg, Germany), and the concentration was taken to be 190 pmol·μl^{-1} as specified by the supplier. The samples were prepared by mixing the 14-mer (2 nmol, 10.5 μL) with an aqueous solution of the complex (1 mg·mL^{-1}) with the appropriate stoichiometry (2, 4, or 10 nmol) and increased to 25 μL with pure water. The samples were maintained at 37 °C for 72 h with vigorous shaking. The ESI measurements were performed on a Micromass Q-Tof Ultima. The samples (5 μL) were desalted at 20 °C by HPLC on a C18 Xterra (Waters, Milford) with a water gradiant of TEAA (triethylammonium acetate) pH 7.9 and an acetonitrile gradient from 0 to 30% in 10 min and to 100% acetonitrile in 5 min; the flow rate was 10 μL/min. Directly after the column, the samples were diluted in two volumes of acetonitrile and injected in the mass spectrometer. The spectra were recorded in negative mode, and before every series of measurements the spectrometer was calibrated with H_3PO_4. The source temperature was set at 373 K and the cone voltage to 35 keV, with a mass range from 400 to 2000. The acquisition and the deconvolution of data were performed on a Mass Lynx (version 4.0) Windows XP PC system using the Max Ent Electrospray software algorithm.

Computational Study. All calculations were carried out using density functional theory as implemented in the Gaussian03 package.[47] The B3LYP exchange−correlation energy functional was used with a mixed basis set consisting of the quasirelativistic Stuttgart/Dresden semicore SDD-ECP[48] with a (8s7p6d)/[6s5p3d]-GTO triple-ζ valence basis set on the ruthenium atoms and 6-31+G-(d) on the remaining atoms.

Geometries and wave functions were optimized starting from suitably adapted structures of the crystal structure of RAPTA-C. Proper convergence was verified via frequency analysis. Basis-set

(42) Nanni, P.; De Giovanni, C.; Lollini, P. L.; Nicoletti, G.; Prodi, G. *Clin. Exp. Metastasis* **1983**, *1*, 373.
(43) Mosmann, T. *J. Immunol. Methods* **1983**, *65*, 55.
(44) Alley, M. C.; Scudiero, D. A.; Monks, A.; Hursey, M. L.; Czerwinski, M. J.; Fine, D. L.; Abbott, B. J.; Mayo, J. G.; Shoemaker, R. H.; Boyd, M. R. *Cancer Res.* **1988**, *48*, 589.
(45) Tamura, H.; Arai, T. *Bunseki KagaKu* **1992**, *41*, 13.
(46) Cocchietto, M.; Sava, G. *Pharmacol. Toxicol.* **2000**, *87*, 193.
(47) *Gaussian 03*, Revision B.03; Gaussian, Inc.: Pittsburgh, PA, 2003.
(48) Andrae, D.; Haeussermann, U.; Dolg, M.; Stoll, H.; Preuss, H. *Theor. Chim. Acta* **1990**, *77*, 123.

superposition errors (BSSE) were corrected following Boys and Bernardi.[49] More details and comparison of different computational packages, functionals, and basis sets can be found in ref 32. Visualizations were made using the program MOLEKEL 4.3.

Acknowledgment. We thank the Swiss National Science Foundation, the EPFL, and COST (Switzerland) for financial support. The present work was carried out with contributions from the Laboratory for the Identification of New Antimetastasis Drugs and developed under the COST D20 action.

(49) Boys, S. F.; Bernardi, F. *Mol Phys.* **1970**, *19*, 553.

Supporting Information Available: The crystallographic information file (cif) of complex $\mathbf{5}^+$ as well as a figure showing the NMR numbering scheme and a table of MS data are available free of charge via the Internet at http://pubs.acs.org.

OM0508841